Computers & Geosciences 89 (2016) 107–117

Contents lists available at ScienceDirect

Computers & Geosciences

journal homepage: www.elsevier.com/locate/cageo

Review article

Computational challenges in the analyses of petrophysics using microtomography and upscaling: A review

Jie Liu [a,b,*], Gerald G. Pereira [c], Qingbin Liu [a], Klaus Regenauer-Lieb [d]

[a] School of Earth Sciences and Geological Engineering, Sun Yat-sen University, Guangzhou 510275, China
[b] Guangdong Provincial Key Laboratory of Mineral Resources & Geological Processes, Guangzhou 510275, China
[c] CSIRO Mathematics, Informatics and Statistics, PrivateBag33, Clayton South, VIC 3168, Australia
[d] School of Petroleum Engineering, University of New South Wales, NSW 2052, Australia

ARTICLE INFO

Article history:
Received 23 September 2015
Received in revised form
26 January 2016
Accepted 27 January 2016
Available online 4 February 2016

Keywords:
Microtomography
Petrophysics
Upscaling
Computations

ABSTRACT

Microtomography provides detailed 3D internal structures of materials in micro- to tens of nano-meter resolution and is quickly turning into a new technology for studying petrophysical properties of rocks. An important step is the upscaling of these properties as micron or sub-micron resolution can only be achieved on the sample-scale of millimeters or even less than a millimeter. We have developed a computational workflow for the analysis of microstructures including the upscaling of material properties. Computations of properties are first performed using conventional material science simulations at micro to nano-scale. The subsequent upscaling of these properties is done by a novel renormalization procedure based on percolation theory. In this paper we discuss the computational challenges arising from the workflow, which include: 1) characterization of microtomography for extremely large data sets; 2) computational fluid dynamics simulations at pore-scale for permeability estimation; 3) solid mechanical computations at pore-scale for estimating elasto-plastic properties; 4) Extracting critical exponents from derivative models for scaling laws. We conclude that significant progress in each of these challenges is necessary to transform microtomography from the current research problem into a robust computational big data tool for multi-scale scientific and engineering problems.

Contents

* Corresponding author at: School of Earth Sciences and Geological Engineering, Sun Yat-sen University, Guangzhou 510275, China.
E-mail addresses: liujieigcea@gmail.com, liujie86@mail.sysu.edu.cn (J. Liu).

http://dx.doi.org/10.1016/j.cageo.2016.01.014
0098-3004/

1. Introduction

Microtomography provides detailed 3D internal structures of materials in micro- to tens of nano-meter resolution and is quickly turning into a new technology for studying petrophysical properties of rocks. Such high resolution can only be achieved on the sample-scale of millimeters or even less than a millimeter, thus to scale up the properties from micro-scale to macro-scale is essential. Consequently this problem is the subject of many microtomography studies (Arns et al., 2001, 2002; Knackstedt et al., 2006; Fredrich et al., 2006; Chai et al., 2010; Derzhi et al., 2010; Grader et al., 2010; Liu and Regenauer-Lieb, 2011; Liu et al., 2014, 2015; Dernaika et al., 2015). The available literature has provided an in-depth account of the basic theory and methodology underpinning the upscaling workflows. However, computational issues arising from big data of microtomography, intensive computations of petrophysics and upscaling, and appropriate strategies for dealing with this challenge have not been discussed yet.

These computational issues include (but are not limited to): 1) characterization of microstructures of very large data – how to characterize, how large are the data sets we can handle, and how fast is the procedure; 2) determination of the size of a representative volume element (RVE) – the size of RVE sets the quanta of computations of properties and the procedure of determination may be very time consuming itself, thus the reliability, complexity and computing costs of the methods must be considered; 3) computations of petrophysical properties – the key problems are which method is used, how accurate the method is and how much it costs in computing resources; 4) extracting critical exponents for upscaling based on percolation theory – there are similar problems to the computations of properties and some additional problems related to the critical model of percolation where the connectivity, such as the width of the channel for fluid flow, is very small. The determination of the size of RVE is a relatively important issue related to the methodology and theory. As we are concerned here with the computational aspects we refer to the cited literature and focus on the problems related to the computations of properties and upscaling. We will also give a brief description about current capability of the characterization of microstructures. Readers that are interested in the topic of RVE size can refer to relevant contributions (Kanit et al., 2003; Terada et al., 2000; Liu et al., 2009; Regenauer-Lieb et al., 2013a). We refer to the same literature for the discussion of the upscaling methodologies which is a complex and much debated issue. It is beyond the scope of this paper, which restricts itself to the important computational problems related to the percolation theory.

While the process described is generic we will discuss derivation of upscaled properties such as permeability, elastic modulus and Poisson's ratio, plastic yielding stress, electrical conductivity. More efforts have been focussed on the analyses of permeability and elastic properties, and less on plastic properties.

Fluid transport and elastic properties have been studied with respect to consideration of microtomographic characterization (Roberts and Garboczi, 2002; Arns et al., 2002, 2005; Knackstedt et al., 2006; Moreno-Atanasio et al., 2010; Lopez et al., 2012; Dvorkin et al., 2012; Shulakova et al., 2013). Numerical methods such as the finite element method (FEM) (Arns et al., 2002; Shulakova et al., 2013), random walk methods, network models (Blunt et al., 2002; Pereira, 1999), smoothed particle hydrodynamics (SPH) (Pereira et al., 2011,2012) and Lattice–Boltzmann (LB) methods (Chai et al., 2010; Narvaez et al., 2010; Ahrenholz et al., 2008; Pan et al., 2006) have been used in the past. Numerical computations on microtomographic data have shown good agreement, to some extent, with experimental data for fluid flow and elastic properties (Arns et al., 2001, 2002, 2005; Knackstedt et al., 2006; Fredrich et al., 2006). New methods have been presented for the derivation of scaling relationships of plastic properties based on percolation theory as well as entropic uncertainty principles which provide sound theoretical bounds for the upscaling of properties from microtomographic data (Liu et al., 2012, 2015; Regenauer-Lieb et al., 2013a, 2013b).

Scientific and technical applications were fully discussed in these publications. Computational and technical aspects have, however, not yet been described. In this contribution, we are concerned with the challenges related to the computations in studying petrophysics and upscaling from microtomographic data. Computational challenges primarily stem from the enormous data size of microtomography. Highly configured computers and parallelized computing are essential but not enough. We introduce here the problems/difficulties and the computational solutions/expectancy based on our practical experience.

An important prerequisite in our approach is that the suggested solutions need to be fully scalable as we anticipate a dramatic increase in computational challenge for future developments. These include amongst others – time-lapse X-Ray microtomography data, significantly larger cameras, data fusion with state-of-the-art equipment such as Focus Ion Beam Scanning Electron Microscope FIB-SEM, Transmission Electron Microscope TEM, Saturated Excitation SAX Microscope, Electron Microscope EMP, more images from nano- to centimeter scales are available. In addition, the computational workflows should be designed as modules for a cyber-infrastructure including data assimilation techniques through mathematical forward and inverse modelling for the upscaling from nano- to reservoir scale. The following workflow and computational approach is designed to tackle current challenges as a preparation for future developments.

2. Workflow and computational methods

Before going into the description of the computational approach we need to summarise the workflow and associated computational method used (Fig. 1). For a complete description and worked examples we refer to the literature (Liu and Regenauer-Lieb, 2011; Regenauer-Lieb et al., 2013a, 2013b; Liu et al., 2014, 2015). A prerequisite to all X-Ray microtomography is segmentation, which in the discussed examples resolves a binary spatial database of pores and solid from gray-scale microtomography images. Andrä et al. (2013a) gave a through introduction and comparison of the techniques of image processing and segmentation. After segmentation is performed the starting model for the following analysis is a digital rock equivalent. This digital rock equivalent is then analyzed in three main components of the workflow. The processing of the segmented binary data is grouped in the left, middle and right columns.

The left column deals with a geometrical analysis, which accomplishes the characterization of geometry (of pores) of the model. Stochastic analyses are also carried out and its outputs are probabilities of porosity, percolation and anisotropy of different sized samples (Liu et al., 2009). The size of a representative volume

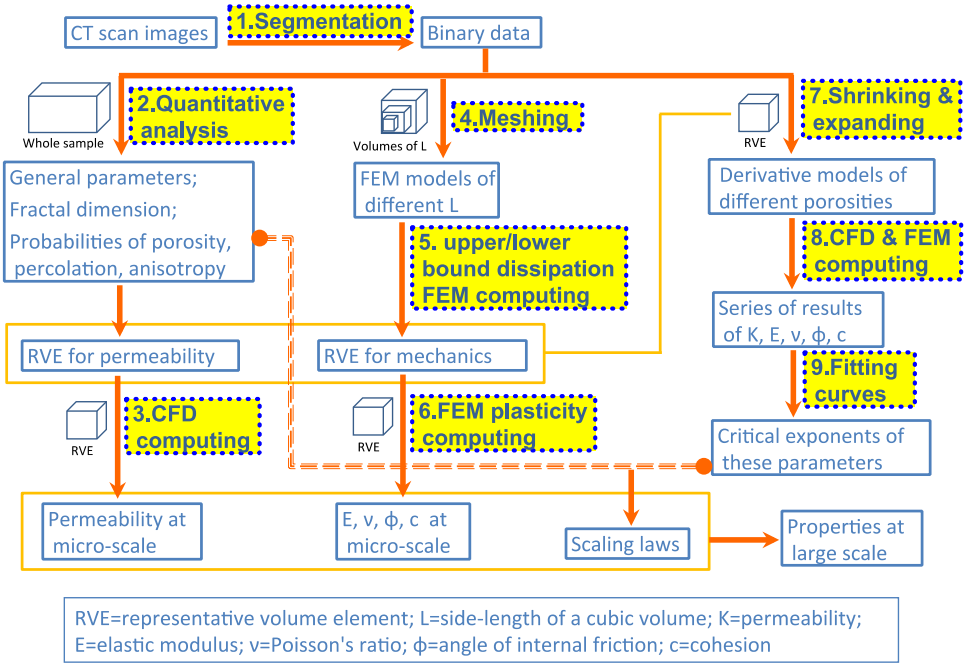

Fig. 1. Workflow of analyzing petrophysics and upscaling from microtomography.

element (RVE) can be determined when the probabilities converge (while the size of the analyzed volume is increasing). Permeability is simulated on RVEs by using computational fluid dynamics (CFD).

The middle column deals with the mechanical analysis. We determine the size of a mechanical RVE by detecting the mechanical responses of maximum and minimum (upper and lower bounds) entropy production on models of different size (Terada et al., 2000; Regenauer-Lieb et al., 2010). Elastic properties, including elastic modulus, shear modules and Poisson's ratio, are detected at the same time. Plastic properties, such as yield stress, cohesion and the angle of friction, can be defined further over the mechanical RVEs.

The right column is concerned with the extraction of critical exponents for scaling laws. Based on percolation theory, parameters such as permeability K, elastic modulus E and yield stress σ_y are predicted to change exponentially as the porosity approaches the percolation threshold with the form of $K=(p-p_c)^{\chi}$, $E=(p-p_c)^{f}$, $\sigma_y=(p-p_c)^{T_f}$, where p is volume fraction and p_c is the percolation threshold (Sieradzki and Li, 1986; Benguigui et al., 1987; Stauffer and Aharony, 1994; Sahimi, 1998). The exponential indicies χ, f and T_f describing this limiting behavior are called critical exponents. We use a shrinking/expanding algorithm (Liu and Regenauer-Lieb, 2011) to create a series of derivative models with different volume fractions p and to detect the percolation threshold p_c. Corresponding parameters of the derivative models close to the percolation threshold are computed, and the critical exponents are fitted. These critical exponents describe the scale-independent features of properties that are changing with volume fraction. With any two critical exponents and/or the fractal dimension, scaling laws are defined.

The nine steps of implementations in the workflow are all computationally intensive. We will discuss steps 2, 3, 6 and 8 in this paper, where computations fall into three categories.

The first category is the characterization of microstructures, or the way to describe microstructures. There are different ways to describe microstructures. Some parameters are commonly used in characterization, such as porosity, connectivity, specific surface area, and orientations. Some specific structures or parameters need special methods to characterize, such as tortuosity (Ghanbarian, et al., 2013) and network model (Dong, 2007; Blunt et al., 2013).

The second category is the simulation of fluid flow at the pore-scale. There are many methods available to use, including lattice-Boltzmann (LB) method, finite difference method (FDM), finite volume method (FVM), smoothed particle hydrodynamics (SPH) method, finite element method (FEM) (Gingold and Monaghan, 1977; Anderson, 1995; Martys and Chen, 1996; Chen and Doolen, 1998; Kandhai et al., 1998; Versteeg and Malalasekera, 2007; Meakin and Tartakovsky, 2009). Among these methods, the finite element method is not frequently used for fluid flow problems, LB method is the most popular method used for fluid flow at pore-scale. As a new technique, the SPH method attracts a lot of interests with important progress in recent year (Tartakovsky et al., 2007; Meakin and Tartakovsky, 2009). The SPH calculations are aimed at characterizing the microphysical processes with pore-scale fluid flow simulations. In the implementations 3 and 8 (see Fig. 1), the simulations of computational fluid dynamics (CFD) are carried out for RVEs of original models and the derivative models by shrinking or expanding structures in RVEs.

For the third category – the computations of mechanical properties, there are different methods available to compute elastic properties, including the finite element method (Garboczi et al., 2001), finite difference method (Andrä et al., 2013b), the dynamic pulse propagation approach (Saenger, 2008), and an elastic solver based on the Lippmann- Schwinger equation (Moulinec and Suquet, 1998). To compute plastic parameters, the former two methods are commonly used and the finite element method is preferred. Calculations are carried out for RVEs of the original digital rock model as well as for derivative models by shrinking or expanding the microstructures contained within the RVEs. The generation of the finite element mesh is a challenging task for the finite element method.

3. Computational challenges

The computational challenges contained in the workflow

(Fig. 1) are a consequence of the large quantity of data and the file size of the high resolution tomograms. The size of microtomographic data can be in the order of (1–9) × 1000^3 voxels. Assuming one voxel corresponds to one hexahedral element, there would be tens of millions to tens of billions of elements. Furthermore, the microstructure of porous rock is by default extremely complex. Efficiently dealing with the complexity of the material is the main computational challenge.

3.1. Characterization of microstructures

There is no standard in the characterization of the microstructure as the software development has been driven by a problem oriented approach which led to the development of custom solutions for different applications. Various methods and software packages have been developed, including open sourced programs and commercial packages such as 3DMA-rock, ImageJ (or FIJI), scanIP, Blob3D (and the family), Avizo[1] and more. The most popular parameters of characterization are: volume fraction (porosity), specific surface area (SSA), the connectivity of the network (or percolation), the size, shape and orientation of individual structures (aspect ratio can be derived), pore size distribution or particle size distribution (PSD).

Among these available tools, Avizo®, a commercial software package originally developed as a data analysis tool for life and material sciences at the Zuse Institute Berlin, is currently the most popular tool to process microtomographic images of rock specimens. In addition to the advanced capabilities of image processing and visualization, Avizo® also has the capability of characterization providing parameters such as porosity, connectivity, size and shape of individual structures. However, the design focus of the package is for industrial use and, it is consequently not suitable for extremely large data sets. Large volumes, i.e. $> 1000^3$ voxels are extremely challenging for Avizo®. Our experience is that we could not use the package for characteristic parameters for volumes larger than 1000^3, no matter how powerful the computer is.

At present, a standard dataset of synchrotron microtomography is 2048^3. It is therefore not practical to use Avizo® to analyze the full dataset of the high resolution tomograms. Moreover, we have recently begun the analysis of 4D data, comprising a series of high resolution scans of three-dimensions (3D) over time. For example, a gypsum sample was heated and scanned in-situ in synchrotron and we got 7 steps of images. In another synchrotron experience, we heated a granite sample to 395 °C and scanned it in every 15 °C, thus we got 26 steps of images. To characterize these 4D data is extremely challenging. As a quickly developing technology, the resolution of microtomography and scanning scope are both increasing. It is anticipated that in the near future a standard dataset of microtomography will be 4096^3. It will be a big challenge to characterize a series, even for just ten steps, of 4D data of this volume.

We have developed an in-house Fortran program, CTSTA (Liu et al., 2013), which addresses the characterization challenge. CTSTA can extract parameters of the characteristics of a full dataset quickly, i.e., in roughly half an hour for a volume of 2048^3. Using this specific tool, we have analyzed the characterization of the heated gypsum sample and granite sample. The results of gypsum sample were reported in Fusseis et al. (2012a). Some results of granite sample were reported in an EGU poster (Fusseis et al., 2012b). We illustrate the original CT images and created microcracks after heating in Fig. 2 and show the statistical results for the frequency of isotropy index of pores and cracks in Fig.3.

The strategy to tackle the challenge of characterization and interpretation at this scale is to perform the analysis without the use of a graphical interface. CTSTA program can run on an ordinary PC, workstation or supercomputer. Its present performance is very fast so that there is no requirement to parallelize it yet. The amount of shared memory of the machine constrains the size of the volume that can be analyzed. We estimate for volumes of 4096^3 a memory need of 96 GB RAM or more. The code of CTSTA is available in (https://github.com/Liujie-SYSU/CTSTA) and an example is provided.

3.2. Simulations of fluid flow

The ability to model fluid passing through a pore-network is the key parameter for reservoir engineering as it leads to the estimation of permeability and is therefore one of the most frequent engineering objectives of microtomographic studies. The advantage of a microtomography technique over the standard laboratory technique is the additional insight gained by the possibility of studying the scaling relationship between the detailed microstructure of pores and permeability. For the simulation of fluid flow at pore-scale, the governing equations are the Navier-Stokes equations. Considering cases where the flow is very slow the simplified Stokes equation can be used as well (Acheson, 1990; Chai et al., 2010; Blunt et al., 2013). Using microtomographic data, generally we compute the velocity of fluid in the pore network, and then the permeability K is calculated from Darcy's equation $K = -(\eta L/\Delta p)\bullet u$, where η is the viscosity of the fluid, L is the length of the model in the analyzed direction, Δp is the hydraulic pressure difference along L, and u is the average superficial velocity in this direction.

Various methods can be used to compute the fluid flow velocity in pore networks as mentioned in Section 2. A full comparison of all different methods has not been done yet. In the following we summarise results from the Lattice–Boltzmann (LB) method and the Smooth-Particle-Hydrodynamics (SPH) method.

3.2.1. Computing cost and accuracy

For a model comprised of voxels, the LB method directly uses vertices of voxels of microtomographic images to define lattice sites; while SPH fills the fluid domain with SPH particles – the more particles per unit volume the higher the accuracy which will be obtained. For SPH the required goal of one particle per voxel has steep computational costs. Pereira et al. (2012) have compared the computing cost of the LB and SPH methods. In testing a model of 100^3 voxels, there are 101^3 lattice sites and ~0.5 million particles were used. The CPU-time of the LB method was around 15 minutes and SPH was 3 days. Apparently, the LB method is much more efficient than the SPH method. The authors also compared the accuracy of the two methods, results are shown in Table 1. There are 3 different structures created by arbitrarily distributed spherical grains, and each of the 3 models was split into 2 resolutions, forming models of 100^3 and 200^3 voxels. We see that the values of permeability computed by using LB method and SPH method are quite different. For the models of 100^3 voxels, it seems values from the LB method is greater than those from SPH, while for the models of 200^3 voxels, it is reverse. Thus we cannot say which method overestimates and which one underestimates permeability.

Considering the Table 1 comparison in computing speed, we selected the LB method to carry out the computations of fluid flow at pore-scale for our carbonate samples (Liu et al., 2014). Two samples with image porosity of 17.56% and 19.60% were analyzed, and the sizes of RVEs are 250^3 to 500^3 voxels, respectively. These

[1] 3DMA-rock (http://www.ams.sunysb.edu/~lindquis/3dma/3dma_rock/3dma_rock.html), ImageJ (or FIJI, http://fiji.sc/Fiji), scanIP (https://www.simpleware.com/software/scanip/), Blob3D (and the family, http://www.ctlab.geo.utexas.edu/software/), Avizo (http://www.fei.com/software/avizo3d/)

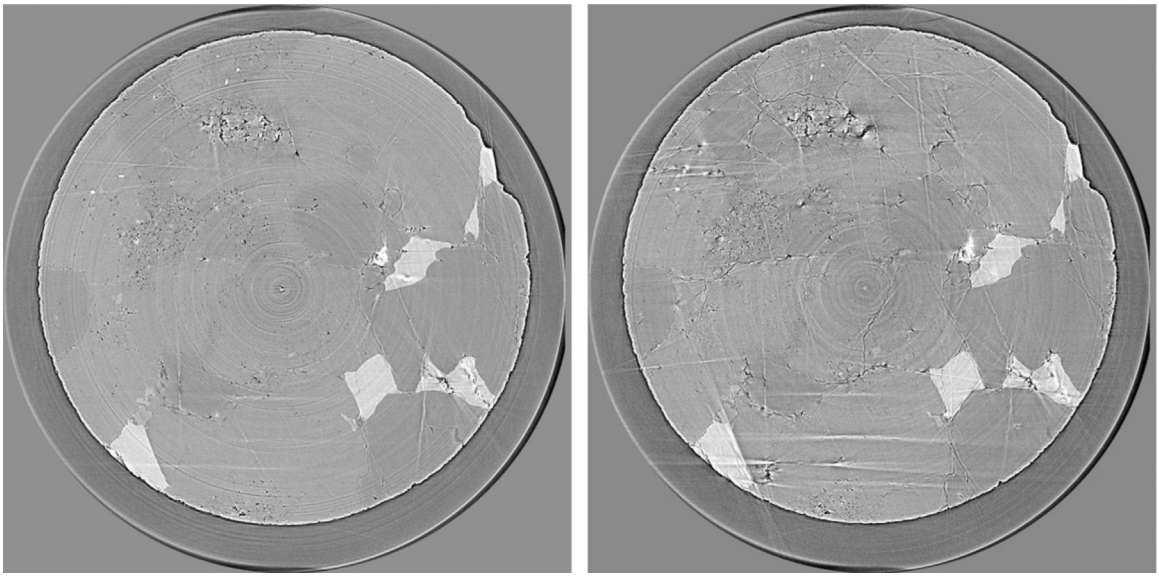

Fig. 2. The same slide of microtomography before (left, 25 °C) and after (right, 335 °C) heating.

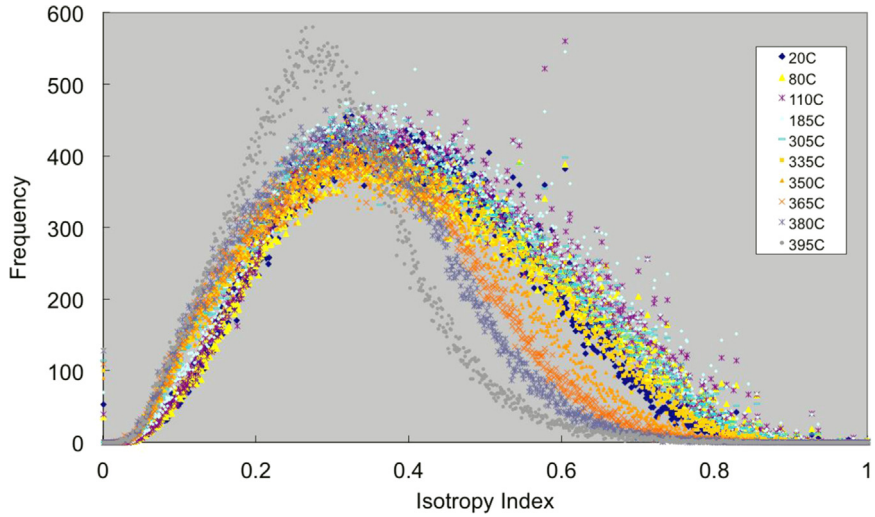

Fig. 3. Histogram of isotropy index of pores and cracks in different temperatures. Isotropy index is defined as the ratio of the minimum and maximum length of a structure. Only a part of the series is presented in figure. The statistical results for frequency of isotropy index after 300 °C shows isotropy index decreasing, representing the development of cracks.

Table 1
Comparison of permeability computed by two methods.

Case	Porosity	100^3 model K (10^{-8} m^2)		200^3 model K (10^{-8} m^2)	
		by LB	by SPH	by LB	by SPH
50 mono-disperse spheres	0.31	1.04	0.25	0.88	1.69
50 mono-disperse spheres	0.38	0.96	0.08	0.75	0.91
25 poly-disperse spheres	0.37	1.51	0.36	1.29	2.51

(Data from Pereira et al., 2012).

two datasets are available via GITHUB (https://github.com/Liujie-SISU/CTdata). The computational time to reach steady state conditions was of the order of a few days (obviously faster for the 250^3 simulations compared to the 500^3 simulations) by using 96 cores. Objectively, 500^3 is not a small volume to compute but is far away from the maximum volume we need to consider. The LB method is recognized as one of fastest CFD tools and has a reputation of very good parallelization. To fulfil computations of larger volumes ($>1000^3$ voxels) in an acceptable time period, it requires massive parallel computing using thousands or more cores on supercomputers. Computations are achievable, but the computing cost is very high.

3.2.2. *Factors affect accuracy*

The computed permeability values are 381.5 and 224.9 mD while the laboratory-measured permeability is 62.1 and 25.6 mD, respectively. The computed permeabilities are larger than laboratory measurement, this situation was also reported by Andrä et al. (2013b). The differences between computed values and measured values are significant but acceptable considering the possible errors both from experiments and simulations (Manwart et al., 2002). The factors that may cause the difference were analyzed (Liu et al., 2014) as: 1) scale – sample sizes used in computing are generally less than 1 mm^3 (250^3 to 500^3 voxels with resolution

around 1.8 μm), while sample sizes used in laboratory are 2 to 3 cm in diameter; 2) heterogeneity – we might have selected high permeability areas to carry out microtomography scan and compute; 3) segmentation – segmentation may not correctly resolve pores and grains for very complex structures.

3.2.3. Requirements for extracting the critical exponent of permeability

For computations to obtain the critical exponent of permeability, the main idea is: based on the RVE, which is the original model, we create a series of models by shrinking or expanding the pore-structure, thus to get derivative models with similar structure but different porosities. From these derivative models, we can detect the percolation threshold p_c, which is the lowest porosity value that exists in a percolating pore-structure (Liu and Regenauer-Lieb, 2011). Here percolating means a pore-structure that connects at least two opposite boundaries of the model. Leaving the critical model (the model with the porosity of p_c) aside, we compute permeability values of the models which are close to and larger than p_c. The group of simulated permeability K values and the porosities p of the models are used to fit χ in $K = (p-p_c)^{\chi}$, which is the critical exponent of permeability. It was suggested that the difference of the porosity from p_c should be less than 0.15; otherwise, the model is not "close to" the percolation threshold (Sahimi, 1998). We can hypothesise that these models have sophisticated channels – as they are close to the critical model, and they do not differ very much from model to model for structure and porosity. This implies that we not only need to compute a series of models, but also need to obtain very accurate results from the series of models with subtle structures. Obviously the demands of computing speed and accuracy for such a task are extremely high.

Our results showed that five derivative models close to the percolation threshold do not give a very good linear relationship of K and $(p - p_c)$ in log–log plots, see in Liu et al. (2014, Fig. 12). Here we show the result of another similar sample in Fig. 4. Five models that are close to the percolation threshold were computed. We used the four points showing good linearity excluding the first one of the smallest $(p - p_c)$ to fit the critical exponent of permeability. Apparently in Fig. 4 the results show correct tendency that permeability increases with porosity. However, the fitted critical exponent of permeability is 0.654, which is quite different from the previous studies based on "bond-shrinkage models" (Wong et al., 1984) and Swiss-cheese models (Halperin et al., 1985). In addition to the difference of models and the strong heterogeneity of our carbonate samples, numerical errors may also cause the difference from the previous studies, to some extent, as the fitted critical exponent is very sensitive to the computed permeability values.

A thorough study needs to compare different models and for each model using different methods. It will be a big investment of research time and computing cost, but definitely worth doing. We expect to see some progress on this problem in near future.

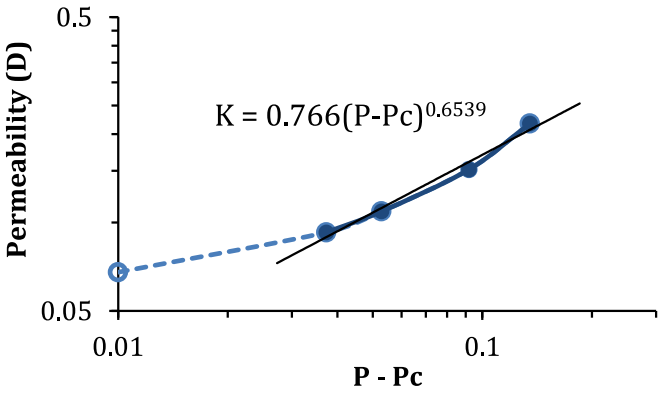

Fig. 4. Fitting the critical exponent of permeability from a series of models with difference porosity.

In summary, for computations of fluid flow at pore-scale to calculate permeability and extract the critical exponent of permeability, current CFD tools and computing facilities are available but the computing cost is rather high. At the same time the accuracy of the computing method is crucial to get reliable critical exponents of permeability for the analysis of upscaling. We are still seeking powerful tools with very high efficiency and accuracy to improve this area of research. Compared to the LB codes which have been around for decades this is a new area of research and huge progress is expected.

3.3. Computations of mechanical properties

The finite element method (FEM) has been used to study the mechanical parameters of rocks. As the most basic mechanical parameters, elastic properties have been studied for over 10 year (Arns et al., 2002; Roberts and Garboczi, 2002; Derzhi et al., 2010; Almqvist et al., 2011; Dvorkin et al., 2012), the study is relatively thorough; while the study of plastic properties has just started (Liu et al., 2012, 2015). The computations of plastic parameters, is still in its infancy and offers huge room for improvements.

3.3.1. General information in plastic computing

To study the plastic properties of rock, we start from the most popular plastic criterion for rocks, Drucker–Prager plasticity. Different from elastic analysis, plastic analysis needs to reach a certain strain value, which generally should be over 0.5%, before the yield stress can be detected. As the yield stress is pressure dependent for Drucker–Prager plasticity, two independent parameters, cohesion and the angle of internal friction, are more commonly used. Cohesion and the angle of friction can be calculated by running two computations of different pressures for the same microstructural model, and based on the linear relationship of Drucker–Prager plasticity $\sigma_y=\sigma_n \tan\beta+c$, where σ_y is the yield stress, σ_n is pressure (or mean stress), c is cohesion, and β is the angle of internal friction. c and β can be determined with two groups of σ_y and σ_n.

In the computations, we assume the parameters of solid part (referring to parameters of minerals) in the microstructural model, and pore-space is treated as void. Averaged stress and strain of all elements of the porous structure are calculated from finite element simulations under certain boundary conditions and used to detect the cohesion and the angle of friction of the microstructural model. We selected the commercial Abaqus® package to perform the finite element computations.

3.3.2. Meshing issues

The first problem we want to discuss is meshing. It is easy to estimate that a model with 200^3 voxels and 20% porosity, there are 64,000,000 elements if one voxel is defined as one hexahedral element. For elastic computations, this number is not a problem with current high performance computing facilities. For plastic computations, it perhaps needs hundreds or even thousands of increments to reach the strain of 0.5%, thus it definitely demands us to reduce elements and speed up computations. Using tetrahedral elements should be an appropriate option. However, it is a challenge to create tetrahedral meshes for very complex microstructures.

Avizo® Fire package was selected to create tetrahedral meshes in our study, which was also used for visualization of microtomography. It can define the maximum length of elements (in voxel side-length), thus define the density of mesh and accuracy of the structure. The package can only create uniform distributed

Table 2
Comparison of models using different meshes and their results.

Element shape	Hexahedron	Tetrahedron	Tetrahedron
Element size	1	2.2	3.26
Number of elements	774,313	1,691,300	522,061
Number of nodes	849,710	312,909	100,760
Distorted elements	0	14	34
Elastic modulus (MPa)	37.72	36.60	36.94
Computing time (s*CPU)	2791*4	338*4	68*4

elements – all elements have similar sizes. Non-uniformly distributed elements – adaptive mesh refinement on the areas of complicated structures and mesh coarsening on the less complicated areas – are not achievable in Avizo®. With complex internal structures, some elements are of very poor quality. Avizo® provides functionalities to improve the quality of individual elements, however, it is not possible to improve all elements to high standards. What we can do is to trade-off of the accuracy of the structure with the number of nodes.

Here we show a comparison of a model of 100^3 voxels, using hexahedral and tetrahedral elements, in computing speed and results of elastic analysis, see Table 2. In fact we have three models of different meshes, one uses hexahedral elements, the other two use tetrahedral elements but with different element sizes (averaged side-length of all elements). Fig. 5 presents two meshes in Table 2, the one using hexahedral elements and the one using tetrahedral elements with the averaged element size of 3.26. Distorted elements are those elements with a bad shape, defined as with a minimum angle between 5° and 12° or maximum angle up to 165°. The computed values of elastic modulus of the three models are very close to each other. Since hexahedral mesh does not modify the model (from images based on voxels), we propose that this model gives us the most accurate result. The models using tetrahedral elements also give very accurate elastic moduli, with errors less than 3%; the computing time decreases dramatically when using tetrahedral elements. It is interesting that the model with the element size of 3.26 gives almost the same result of elastic modulus as the one with the element size of 2.2 – a little higher value does not mean it is more accurate, but should be attributed to computing error. These results indicate that using tetrahedral elements is a satisfactory practice.

3.3.3. Convergence issues

The second problem we want to discuss is the convergence of plastic computation. The computation of plasticity is a static problem (time-independent) from the concept of physics. Therefore the implicit module Abaqus® Standard should be used and the static stress analysis selected. An example of our models is the RVE size of 300^3 voxels. We coarsened the mesh by controlling the maximum length of element to 5.0 voxels and created 2,818,504 tetrahedral elements and 543,914 nodes. Theoretically, Abaqus® Standard can compute a model of this size and using multi-cores can speed up the computation. The reality is, however, that the computing is not only extremely slow, but also not convergent and the computation failed before (much smaller than) the strain of 0.5%.

To overcome the problem of computing speed and convergence, we were forced to use the explicit method of Abaqus® Explicit. The computation completed successfully to the strain of 0.5%. It ran for 4 h and 25 min on 8 cores. We have computed several samples and found that the computing speeds of different models with a similar number of nodes can be quite different. This should be related to the number of the distorted elements and the extent of distortion. It appears that Abaqus® Explicit is a satisfactory tool to perform the plasticity computations of rocks with complex structures based on microtomographic data.

3.3.4. Difficulties in extracting the critical exponent of yield stress

For computations that aim at deriving the critical exponent of yield stress, the main idea is similar to that of the critical exponent of permeability. Based on the mechanical RVE, which is the original model, we create a series of models by shrinking the solid-structure. From these derivative models we detect the percolation threshold p_c of the solid. Then we compute the yield stress values of the models close to and larger than p_c. The group of yield stress and corresponding volume fractions are used to fit T_f in $\sigma_y=(p-p_c)^{T_f}$, which is the critical exponent of yield stress.

In these computations, we encountered again meshing problems. When a model is close to the percolation threshold, the key links are normally very thin. By creating tetrahedral elements the thinnest links are broken, thus a percolating model becomes non-percolating, see Fig. 6.

In this situation, we had to therefore use hexahedral elements where each voxel is equivalent to an element. Accordingly, the

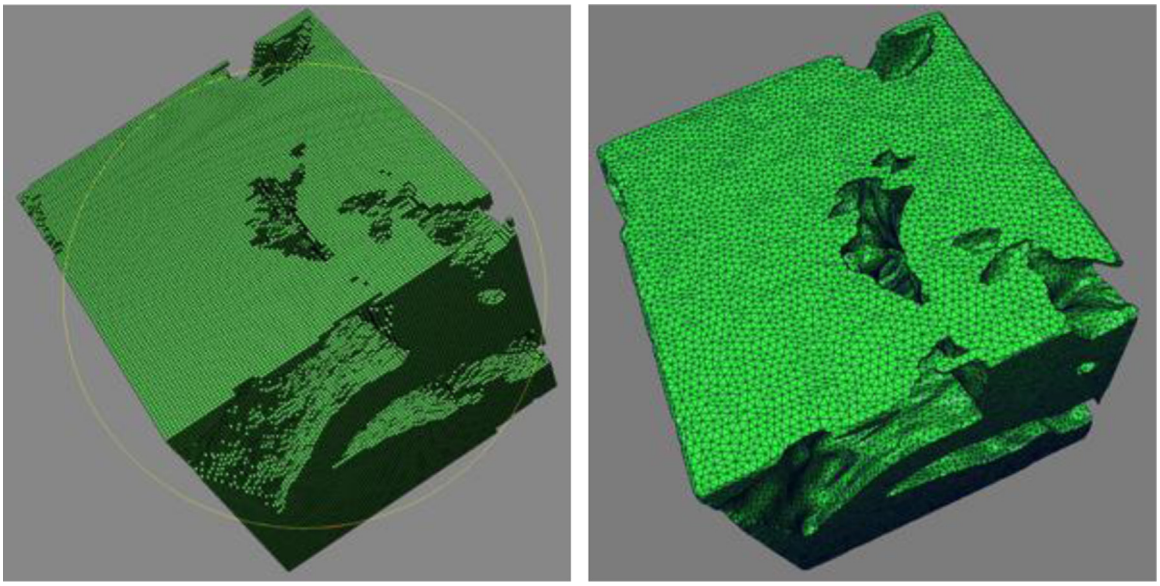

Fig. 5. Comparison of meshes, the one using hexahedral elements (left) and the one using tetrahedral element with the averaged element size of 3.26 (right).

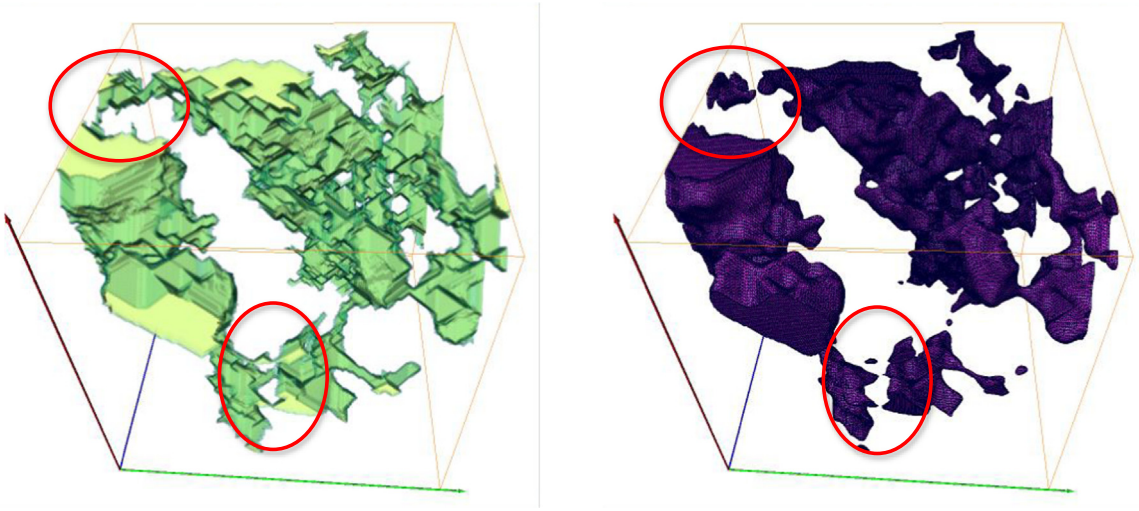

Fig. 6. A percolating model with thin links (left) becomes non-percolating after meshing by tetrahedral elements (right) and thin links are broken.

number of elements and nodes is significant for the computations. There is no limit to the degree of freedom for Abaqus® Standard, but for Abaqus® Explicit, the maximum number of nodes that can be computed is 8 million. The volume fractions of solid of the derivative models close to percolation threshold are generally in the range of 6–26% for our analyzed samples. These derivative models were generated from RVE sizes of 200^3 to 300^3 voxels, thus the number of nodes may exceed the capability of Abaqus® Explicit and some models could not be computed. The maximum number of nodes is of 7,465,946 for our computed model. The computing time is acceptable – using around 35 h on 4 CPUs. The limitation of 8 million-node of Abaqus® Explicit may be outdated for its most recent version.

The performance and accuracy of both the finite element method and finite difference method ensure that the computations related to the critical exponent of yield stress are robust. The obtained exponent and discussions can be found in Liu et al. (2015) and not present here.

3.3.5. Post-processing issues

The next problem is about post-processing of the output data. For the maximum model we analyzed, the output file is about 82 GB, which contains only 20 output steps in 1000 computed steps. It means a large amount of detailed information is not recorded after computing. For the recorded basic information, it is very time consuming to do even simple post-processing of this size. For example, we used a Python script to calculate the average stress and strain values over all elements for the 20 output steps – it took 43.5 h on a single CPU as the script was not parallelized. It is also very hard to open an output file of this size using Abaqus/CAE. On specially configured computers, it can be opened but the processing was too slow to implement and refresh the visualizing steps.

Furthermore, the 3D visualizing capability of the viewer of the finite element package is limited, for example, the internal deformation and distribution of variables can only be seen by slices. Using volume rendering techniques to visualize the output files is an interesting solution. Parallel visualization would help to process very large data sets. Fig. 7 shows a comparison of 3D visualization of plastic strain using Abaqus®/CAE and Paraview. To achieve the visualization, a Python script is written to convert Abaqus ODB file to VTK format that is acceptable for Paraview.

In summary, for computations of mechanical parameters from microtomography and extracting the critical exponent of yield stress, current tools can help us to achieve the analysis but the procedures are not satisfying. To make every step perfect, we are looking for more powerful tools including: 1) good meshing package – to create meshes with much fewer nodes (and degrees of freedom) and keep the subtle structure at the same time; 2) open sourced computing software (finite element or other methods) instead of commercial software – to reduce computing cost; 3) computing software with very good parallelization – to speed up the numerical implementations; 4) huge storage – to store large amount of data; 5) powerful visualization facilities (software and hardware) – to do post-processing and visualization. In addition, for the same reason as for the extraction of the critical exponent of permeability, the computing software must be of very high accuracy to obtain reliable estimates of the critical exponents of yield stress for the analysis of upscaling.

4. Discussion and conclusions

A computational workflow has been developed for the analysis of petrophysics and upscaling by using microtomographic data. Almost every step in the workflow is computing intensive. In this paper we focus on computational challenges involved in the workflow rather than scientific problem of petrophysics and upscaling for the purpose of sharing experience to peers with the same interests, and also calling attention to developing techniques related to these studies. This is an intensive research area in its own right. In addition to our own custom made models for the characterization and statistical evaluation of mictomographic data we have identified areas where codes are mature (LB) and areas where significant improvements are still needed (FEM).

For the characterization of microtomography, our in-house code can analyze parameters such as porosity, connectivity or percolation, specific surface area, particle size distribution or pore size distribution. For each independent structure, its position, size, orientation and dimensions in 3 principal directions can be determined. The advantage of our in-house code is that it can deal with large data quickly, say around half an hour for a 2048^3 full dataset. The maximum volume that can be processed is only limited by the configuration of computer used to run the analyses.

For the computations of fluid dynamics at pore-scale, currently the most popular method is the LB method, which is reputed to have good computing speed and generally reliable precision. However, in spite of the maturity of the codes there is still a strong need for LB with very good parallelization to perform computations of very large volumes, such as 1000^3 voxels (and over), in an

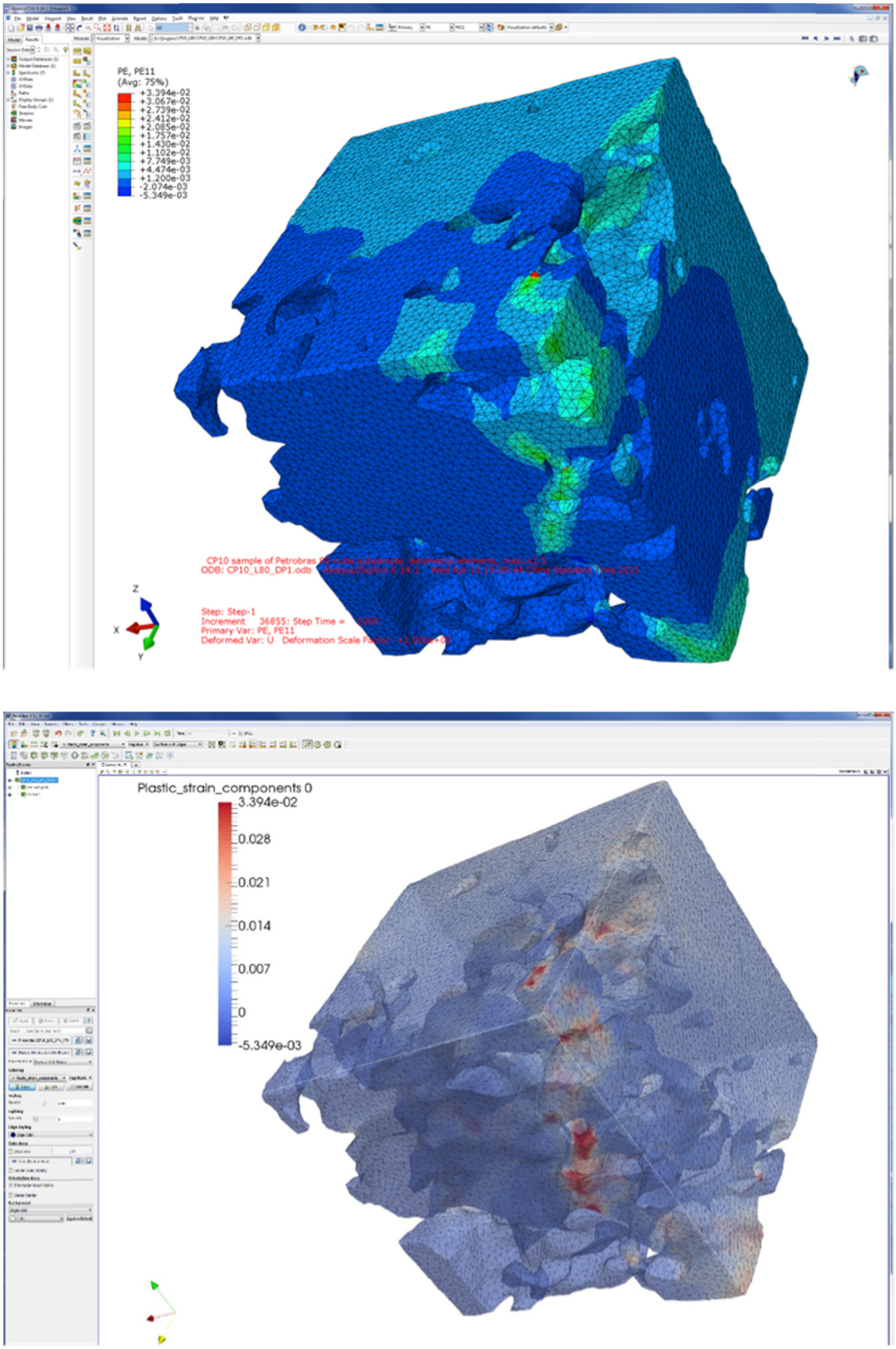

Fig. 7. Visualization using Abaqus/CEA (left) and Paraview (right). High plastic strain values are located inside of the model and volume rendering in Paraview reveals it.

acceptable computing time. These implementations also cannot compromise on very good precision to get more reliable computed permeability. In the case of extracting the critical exponent of permeability, the precision is much more important, because models close to the percolation threshold are delicate and a small change of the computed permeability of each model affects the fitted critical exponent seriously.

For the computations of solid mechanics at pore-scale, the finite element method is commonly used. Meshing algorithms for FEM still need to improve significantly. Based on our analysis, for a low porosity model (lower than 30%) using tetrahedral elements instead of hexahedral elements does not change the computed mechanical parameters much. For example, using tetrahedral elements the error of elastic modulus is less than 5% while computing speed increased 40 times. However, for a high porosity model, such as models close to the percolation threshold of solid, using tetrahedral elements instead of hexahedral elements may cause broken key links and a percolating model becomes non-percolating – the difference between percolating and non-percolating models is vast and cannot be described by errors.

The requirement of meshing is to be able to create meshes with much fewer nodes – to reduce computing cost, and at the same time to keep the subtle structure – to ensure the precision and meaningfulness of the computations. Using uniform hexahedral elements equivalent to voxels keeps the structure exactly but is too expensive for computing; using tetrahedral elements can reduce nodes dramatically but changes the structure. Using non-uniform hexahedral elements should be a solution that could be based on modern graphics approaches such as octree. To the best of our knowledge, there is no suitable meshing package available yet to create non-uniform hexahedral elements automatically for big models with extremely irregular and complex internal structures like porous rocks.

We have used a commercial finite element package to perform the mechanical computations. Difficulties were encountered because of the complicated structures, perhaps also because of the distorted elements, while using a static solver. A dynamic solver resolved the problem and we have reached suitable quasi-static results. To fulfil analyses of a large number of samples, and also consider very large volumes, we require well-parallelized, open sourced programs to perform finite element computations. The same applies to the critical exponent of permeability. Fitting the critical exponent of yield stress needs crucially high precision in the computing of mechanical response. In addition, in order to match the physical concept, a static solver is preferred although a dynamic solver is acceptable.

Related to big data of microtomography, the size of the output files of the CFD and mechanical computations is another challenge. Huge storage is necessary to keep detailed output data. Powerful visualization facilities and software are also necessary to illustrate the distributions of the computed variables.

With high resolution, the sizes of rock samples of microtomography are at the scale of $\sim$1 mm. Petrophysical properties at macro-scale may be different from those derived from this size. Thus the upscaling of properties from microtomography is an issue which must be considered. Some popular methods of upscaling include effective medium theory, computational homogenization, and percolation theory (Guéguen et al., 2006; Regenauer-Lieb et al., 2013a). Effective medium theory is suitable only to predict the properties of statistically homogeneous media at macro-scale (Guéguen et al., 2006). Computational homogenization utilizes numerical methods to derive equivalent values of properties through defining equivalence criteria. This method is adopted in our workflow and embodied in the step 5 “upper/lower bound dissipation FEM computing” (Liu et al., 2012, 2015; Regenauer-Lieb et al., 2013). Percolation theory was originally proposed in statistical physics to describe the global connectivity of randomly heterogeneous systems. It comprises various scaling ideas such as fractal, finite-size scaling, renormalization, and scaling laws. Percolation theory is used to estimate the critical porosity to derive the percolation threshold from natural data and to derive critical exponents and the fractal dimension of the percolating network (Liu and Regenauer-Lieb, 2011; Liu et al., 2012, 2014, 2015). It is relatively well known that the fractal dimension is scale invariant. Critical exponents are similar scale invariants describing scale-independent characteristic of physical properties, including permeability, elastic modulus and yield stress. They are describing the statistical properties of a percolating structure and therefore differ from the classical fractal dimension of a microstructure itself. We would like to point out that: i) the derivation of critical exponents from digital rock images has only become available recently (Liu and Regenauer-Lieb, 2011); ii) they are still at an early stage of investigation, only limited parameters/properties of specific structures have been studied; iii) to extract critical exponents is computationally expensive, as the corresponding property need to be simulated, and computational challenges may be encountered in the simulations.

In conclusion, the analyses of microtomography for petrophysics and upscaling are young fields of research and strong ongoing research topics in computational geosciences. There are some major challenges/problems to overcome. Significant progress in each of these challenges is necessary to transform microtomography from the current research problem into a robust computational big data tool for multi-scale scientific and engineering problems.

Acknowledgment

We are grateful to Petrobras' financial support of this research (iGEM4D) and permission of this publication. We are thankful to Pawsey center of Western Australia for the technical support and access to its visualisation facilities and supercomputers. We thank Ali Karrech in the University of Western Australia and Thomas Poulet in Energy Flagship of CSIRO for their help on finite element computing and pre-/post- processing. We also thank Bjarne Almqvist and an anonymous reviewer for their suggestions on improving the manuscript.

Some later work was supported by “the Fundamental Research Funds for the Central Universities of China (project number: 141gjc12)”.

References

Acheson, D.J., 1990. Elementary Fluid Dynamics, Oxford Applied Mathematics and Computing Science Series. Oxford University Press, New York, ISBN 0-19-859679-0.

Ahrenholz, B., Tolke, J., Lehmann, P., Peters, A., Kaestner, A., Krafczyk, M., Durner, W., 2008. Prediction of capillary hysteresis in a porous material using lattice-Boltzmann methods and comparison to experimental data and a morphological pore network model. Adv. Water Resour. 31, 1151–1173.

Almqvist, B.S.G., Mainprice, D., Madonna, C., Burlini, L., Hirt, A.M., 2011. Application of differential effective medium, magnetic pore fabric analysis, and X-ray microtomography to calculate elastic properties of porous and anisotropic rock aggregates. J. Geophys. Res.: Solid Earth 116, 1–17. http://dx.doi.org/10.1029/2010JB007750.

Anderson, J.D., 1995. Computational Fluid Dynamics: The Basics With Applications. McGraw-Hill Science, New York, ISBN 0-07-001685-2.

Andrä, H., Combaret, N., Dvorkin, J., Glatt, E., Han, J., Kabel, M., Zhan, X., 2013a. Digital rock physics benchmarks—part I: Imaging and segmentation. Comput. Geosci. 50, 25–32. http://dx.doi.org/10.1016/j.cageo.2012.09.005.

Andrä, H., Combaret, N., Dvorkin, J., Glatt, E., Han, J., Kabel, M., Zhan, X., 2013b. Digital rock physics benchmarks—part II: Computing effective properties. Comput. Geosci. 50, 33–43. http://dx.doi.org/10.1016/j.cageo.2012.09.008.

Arns, C.H., Knackstedt, M.A., Pinczewski, W.V., 2001. Accurate estimation of transport properties from microtomographic images. Geophys. Res. Lett. 28 (17), 3361–3364.

Arns, C.H., Knackstedt, M.A., Pinczewski, W.V., Garboczi, E.J., 2002. Computation of linear elastic properties from microtomographic images: Methodology and

agreement between theory and experiment. Geophysics 67 (5), 1396. http://dx.doi.org/10.1190/1.1512785.
Arns, C., Bauget, F., Sakellariou, A., Senden, T.J., Sheppard, A.P., Sok, R.M., et al., 2005. Pore scale characterization of carbonates using X-ray microtomography. SPE J. 2005, 475–484. http://dx.doi.org/10.2118/90368-PA.
Benguigui, L., Ron, P., Bergman, D.J., 1987. Strain and stress at the fracture of percolative media. J. Phys. 48, 1547–1551.
Blunt, M.J., Jackson, M.D., Piri, M., Valvatane, P.H., 2002. Detailed physics, predictive capabilities and macroscopic consequences for pore-network models of multiphase flow. Adv. Water Resour. 25, 1069–1089.
Blunt, M.J., Bijeljic, B., Dong, H., Gharbi, O., Iglauer, S., Mostaghimi, P., Pentland, C., 2013. Pore-scale imaging and modelling. Adv. Water Resour. *51*, 197–216. http://dx.doi.org/10.1016/j.advwatres.2012.03.003.
Chai, Z.H., Shi, B.C., Lu, J.H., Guo, Z.L., 2010. Non-Darcy flow in disordered porous media: a lattice Boltzmann study. Comput. Fluids 39, 2069–2077.
Chen, S., Doolen, G.D., 1998. Lattice Boltzmann Method for Fluid Flows. Annu. Rev. Fluid Mech. 30, 329–364.
Dernaika, M., Uddin, Y. N., Koronfol, S., Al Jallad, O., Sinclair, G., Hanamura, Y., Horaguchi, K., 2015, September 14). Multi-Scale Rock Analysis for Improved Characterization of Complex Carbonates. Society of Petroleum Engineers. http://dx.doi.org/10.2118/175598-MS. 14 September 2015.
Derzhi, N., Dvorkin, J., Diaz, E., Baldwin, C., Fang, Q., Sulayman, A. et al., 2010. Comparison Of Traditional And Digital Rock Physics Techniques To Determine The Elastic Core Parameters In Thamama Formation, Abu Dhabi. Society of Petroleum Engineers. http://dx.doi.org/10.2118/138586-MS. 1 January 2010.
Dvorkin, J., Derzhi, N., Diaz, E., Fang, Q., 2012. Relevance of computational rock physics. Geophysics 76 (5), E141–E153. http://dx.doi.org/10.1190/GEO2010-0352.1.
Dong, H., 2007. Micro-CT image and pore network extraction, PhD thesis, Imperial College, London.
Fredrich, J.T., DiGiovanni, A.A., Noble, D.R., 2006. Predicting macroscopic transport properties using microscopic image data. J. Geophys. Res. 111 (B03201), 1–14. http://dx.doi.org/10.1029/2005JB003774.
Fusseis, F., Schrank, C., Liu, J., Karrech, A., Llana-Fúnez, S., Xiao, X., Regenauer-Lieb, K., 2012a. Pore formation during dehydration of a polycrystalline gypsum sample observed and quantified in a time-series synchrotron X-ray micro-tomography experiment. Solid Earth 3 (2007), 71–86. http://dx.doi.org/10.5194/se-3-71-2012.
Fusseis, F., Schrank, C.E., Liu, J., 2012b. Thermal damage in Westerly granite investigated by means of Synchrotron radiation based microtomography. In: Proceedings of the EGU General Assembly 2012. Vol. 14, p. 12764.
Garboczi, E.J., Berryman, J.G., Livermore, L., 2001. Elastic moduli of a material containing composite inclusions : effective medium theory and finite element computations. Fire Res. 33 (8), 455–470. http://dx.doi.org/10.1016/S0167-6636(01)00067-9.
Ghanbarian, B., Hunt, A.G., Ewing, R.P., Sahimi, M., 2013. Tortuosity in porous media: a critical review. Soil Sci. Soc. Am. J. 77, 1461. http://dx.doi.org/10.2136/sssaj2012.0435.
Gingold, R.A., Monaghan, J.J., 1977. Smoothed particle hydrodynamics-Theory and application to non-spherical stars. Mon. Not. R. Astron. Soc. 181, 375–389. http://dx.doi.org/10.1093/mnras/181.3.375.
Grader, A., Mu, Y., Toelke, J., Baldwin, C., Fang, Q., Carpio, G. et al., 2010. Estimation of Relative Permeability Using the Lattice Boltzmann Method For Fluid Flows, Thamama Formation, Abu Dhabi. Society of Petroleum Engineers. http://dx.doi.org/10.2118/138591-MS. 1 January 2010.
Guéguen, Y., Ravalec, M. Le, Ricard, L., 2006. Upscaling: Effective Medium Theory, Numerical Methods and the Fractal Dream. Pure App. Geophys. 163 (5–6), 1175–1192. http://dx.doi.org/10.1007/s00024-006-0053-y.
Halperin, B.I., Feng, S., Sen, P.N., 1985. Differences between lattice and continuum percolation transport exponents. Phys. Rev. Lett. 54, 2391–2394.
Kandhai, D., Vidal, D.J.-E., Hoekstra, A.G., Hoefsloot, H., Iedema, P., Sloot, P.M.A., 1998. A comparison between lattice_Boltzmann and finite-element simulations of fluid flow in static mixer reactor. Int. J. Modern Phys. 9, 1123–1128.
Kanit, T., Forest, S., Galliet, I., Mounoury, V., Jeulin, D., 2003. Determination of the size of the representative volume element for random composites: Statistical and numerical approach. Int. J. Solids Str. 40 (13–14), 3647–3679. http://dx.doi.org/10.1016/S0020-7683(03)00143-4.
Knackstedt, M.A., Arns, C.H., Saadatfar, M., Senden, T.J., Limaye, A., Sakellariou, A. et al., 2006. Elastic and transport properties of cellular solids derived from three-dimensional tomographic images. In: Proceedings of the Royal Society A: Mathematical, Physical and Engineering Sciences, 462, 2833–2862. http://dx.doi.org/10.1098/rspa.2006.1657.
Liu, J., Regenauer-Lieb, K., Hines, C., Liu, K., Gaede, O., Squelch, A., 2009. Improved estimates of percolation and anisotropic permeability from 3-D X-ray microtomography using stochastic analyses and visualization. Geochem. Geophys. Geosyst. 10. http://dx.doi.org/10.1029/2008GC002358.
Liu, J., Regenauer-Lieb, K., 2011. Application of percolation theory to microtomography of structured media: Percolation threshold, critical exponents, and upscaling. Phys. Rev. E – Stat. Nonlinear Soft Matter Phys. 83, 1–13. http://dx.doi.org/10.1103/PhysRevE.83.016106.
Liu, J., Freij-Ayoub, R., and Regenauer-Lieb, K., 2012. Determination of the plastic strength of carbonates from microtomography and upscaling using percolation theory. In: Proceeding of ECCOMAS 2012, (Ed. J. Eberhardsteiner et al.), Vienna, Austria, September 10–14, 2012.
Liu J., Regenauer-Lieb K., Hines C., Zhang S., Bourke P., Fusseis F., Yuen D., 2013, Applications of microtomography to multi-scale system dynamics – visualisation, characterisation and high performance computation, In: GPU Solutions to Multi-scale Problems in Science and Engineering, Springer-Verlag Lecture Notes in Earth System Sciences, (Ed., Yuen et al.), pp. 617–638.
Liu, J., Pereira, G.G., Regenauer-Lieb, K., 2014. From characterisation of pore-structures to simulations of pore-scale fluid flow and the upscaling of permeability using microtomography: a case study of heterogeneous carbonates. J. Geochem. Explor. 144, 84–96. http://dx.doi.org/10.1016/j.gexplo.2014.01.021.
Liu, J., Freij-Ayoub, R., Regenauer-Lieb, K., 2015. Rock Plasticity from Microtomography and Upscaling. J. Earth Sci. 26 (1), 053–059. http://dx.doi.org/10.1007/s12583-015-0520-4.
Lopez, O., Mock, A., Oren, P.E., Long, H., Kalam, Z, Vahrenkamp, V., et al., Vizamora, A., 2012. Validation of fundamental carbonate reservoir core properties using digital rock physics. SCA2012-19, presented at the International Symposium of the Society of Core Analysts held in Aberdeen, Scotland, UK, 27–30 August, 2012.
Manwart, C., Aaltosalmi, U., Koponen, A., Hilfer, R., Timonen, J., 2002. Lattice-Boltzmann and finite-difference simulations for the permeability for three-dimensional porous media. Phys. Rev. E. 66, 016702.
Meakin, P., Tartakovsky, A., 2009. Modeling and simulation of pore-scale multiphase fluid flow and reactive transport in fractured and porous media. Rev. Geophys. 2008, 1–47. http://dx.doi.org/10.1029/2008RG000263.1.INTRODUCTION.
Moreno-Atanasio, R., Williams, R.A., Jia, X., 2010. Combining X-ray microtomography with computer simulation for analysis of granular and porous materials. Particuology 8, 81–90.
Martys, N.S., Chen, H., 1996. Simulation of multicomponent fluids in complex three dimensional geometries by the lattice Boltzmann method. Phys. Rev. E 53, 743–750.
Moulinec, H., Suquet, P., 1998. A numerical method for computing the overall response of nonlinear composites with complex microstructure. Comput. Methods Appl. Mech. Eng. 157 (1–2), 371–390.
Narvaez, A., Zauner, T., Raischel, F., Hilfer, R., Harting, J., 2010. Quantitative analysis of numerical estimates for the permeability of porous media from lattice-Boltzmann simulations. J. Stat. Mech: Theory Exp., P11026. http://dx.doi.org/10.1088/1742-5468/2010/11/P11026.
Pan, C.X., Luo, L.S., Miller, C.T., 2006. An evaluation of lattice Boltzmann schemes for porous medium flow simulation. Comput. Fluids 35, 898–909.
Pereira, G.G., 1999. Numerical pore-scale modeling of three-phase fluid flow: comparison between simulation and experiment. Phys. Rev. E 59, 4229–4242.
Pereira, G.G., Prakash, M., Cleary, P.W., 2011. SPH modeling of fluid at the grain level in a porous medium. Appl. Math. Model. 35, 1666–1670.
Pereira, G.G., Dupuy, P.M., Cleary, P.W., Delaney, G.D., 2012. Comparison of permeability of model porous media between SPH and LB. Prog. Comput. Fluid Dyn. 12, 176–186.
Regenauer-Lieb, K., Karrech, A., Chua, H., Horowitz, F., Yuen, D., 2010. Time-dependent, irreversible entropy production and geodynamics. Philos. Trans. R. Soc. Lond. A 368, 285–300.
Regenauer-Lieb, K., Veveakis, M., Poulet, T., Wellmann, F., Karrech, A., Liu, J., Trefry, M., 2013a. Multiscale coupling and multiphysics approaches in earth sciences: Theory. J. Coupled Syst. Multiscale Dyn. 1 (1), 49–73. http://dx.doi.org/10.1166/jcsmd.2013.1012.
Regenauer-Lieb, K., Veveakis, M., Poulet, T., Wellmann, F., Karrech, A., Liu, J., Hauser, J., Schrank, C., Gaede, O., Fusseis, F., Trefry, M., 2013b. Multiscale couping and multiphysics approaches in earth science: applications. Theory. J. Coupled Syst. Multiscale Dyn. 1 (3), 281–323. http://dx.doi.org/10.1166/jcsmd.2013.1021.
Roberts, a P., Garboczi, E.J., 2002. Elastic properties of model random three-dimensional open-cell solids. J. Mech. Phys. Solids 50 (1), 33–55. http://dx.doi.org/10.1016/S0022-5096(01)00056-4.
Saenger, E.H., 2008. Numerical methods to determine effective elastic properties. Int. J. Eng. Sci. 46, 598–605. http://dx.doi.org/10.1016/j.ijengsci.2008.01.005.
Sahimi, M., 1998. Non-linear and non-local transport processes in heterogeneous media: from long-range correlated percolation to fracture and materials breakdown. Phys. Rep. 306, 213–395.
Shulakova, V., Pervukhina, M., Müller, T.M., Lebedev, M., Mayo, S., Schmid, S., Gurevich, B., 2013. Computational elastic up-scaling of sandstone on the basis of X-ray micro-tomographic images. Geophys. Prospect. 61 (2), 287–301. http://dx.doi.org/10.1111/j.1365-2478.2012.01082.x.
Sieradzki, K., Li, R., 1986. Fracture behavior of a solid with random porosity. Phys. Rev. Lett. 56, 2509–2512.
Stauffer, D., Aharony, A., 1994. Introduction to percolation theory, Second ed. Taylor & Francis Ltd, London.
Tartakovsky, A.M., Meakin, P., Scheibe, T.D., Wood, B.D., 2007. A smoothed particle hydrodynamics model for reactive transport and mineral precipitation in porous and fractured porous media. Water Resour. Res. 43 (5), 1–18. http://dx.doi.org/10.1029/2005WR004770.
Terada, K., Hori, M., Kyoya, T., et al., 2000. Simulation of the multi-scale convergence in computational homogenization approaches. Int. J. Solid Str. 37, 2285–2311.
Versteeg, H.K., Malalasekera, W., 2007. An Introduction to Computational Fluid Dynamics: The Finite Volume Method, 2nd Edition, Pearson Education Limited, New York, ISBN: 0131274988.
Wong, P., Koplik, J., Tomanic, J.P., 1984. Conductivity and permeability of rocks. Phys. Rev. B 30, 6606–6614.